

# Evaluation of Factors-of-Interest in Bone Mimicking Models Based on DFT Analysis of Ultrasonic Signals

Aleksandrs Sisojevs<sup>a</sup>, Alexey Tatarinov<sup>b</sup> and Anastasija Chaplinska  
*Institute of Electronics and Computer Science, 14 Dzerbenes Str., Riga, Latvia*

**Keywords:** Pattern Recognition, DFT, Bone Models, Axial Quantitative Ultrasound.


**Abstract:** Bone fragility in osteoporosis is associated with a decrease in the thickness of the cortical layer CTh in long bones and the development of internal porosity P in it. In the present work, an attempt was made to predict the factors-of-interest CTh and P based on the pattern recognition approach, where DFT analysis was applied to ultrasonic signals in surface transmission through a soft tissue layer. Compact bone was modeled with PMMA plates with gradual changes in CTh from 2 to 6 mm, and internal porosity P was created by drilling where the thickness of the porous layer P varied from 0 to 100% of CTh. The estimation method was based on a statistical analysis of the magnitude of the DFT spectrum of the ultrasonic signals. Decision rules were mathematical criteria calculated as ratios between the envelope functions of the magnitudes. Each of the objects was chosen in turn as a test object, while other specimens composed the training set. The results of the experiments showed the potential effectiveness of the CTh and P prediction, while additional physical parameters may be used as decision rules to improve the reliability of the diagnosis.


## 1 INTRODUCTION

Osteoporosis is a systemic skeletal disease characterized by low bone density and microarchitectural deterioration of bone tissue with a consequent increase in bone fragility (WHO, 2003). It is a severe symptom of aging and a complication in many metabolic diseases. Cortical bone or compact bone tissue, the main load-carrying component of the skeleton, suffers from osteoporosis by reducing the thickness of the compact layer and increasing the internal porosity in it, progressing from the side of the channel (Osterhoff et al., 2016). An adequate assessment of these manifestations of osteoporosis can help in timely prevention and treatment. Conventionally, the diagnosis of osteoporosis is made using dual x-ray absorption techniques by measuring the bone mineral density (Guglielmi, 2010). However, planar radiography is not able to distinguish reliably between changes associated with bone thinning and porosity and thus distinguish between thin normality and osteoporosis.

Ultrasonic techniques based on measuring the parameters of elastic waves are a perspective

modality to assess bone conditions in respect of osteoporosis (Laugier, 2008). Axial bone ultrasonometers use to measure ultrasound velocity in the compact bone of long bones, such as the tibia and forearm bones. Although it demonstrated sensitivity to osteoporosis and mineralization disorders, its clinical use is compromised by the inability to discern multiple factors influencing the bone condition by this single input. New approaches are focused on analysing guided wave propagation at several frequencies that provide extensive information about bone structure and properties (Tatarinov et al., 2014). However, discrimination of the factors of interest such as cortical porosity and thickness of the cortical layer against the background of the influence of the surrounding soft tissues requires advanced data processing. Traditional approaches based on the measurement of single parameters such as ultrasound velocity do not allow separating the complex influences of these acting factors. Artificial intelligence methods, particularly, pattern recognition applied to a complex of propagated ultrasonic signals at different frequencies are expected to help solve the problem.

<sup>a</sup>  <https://orcid.org/0000-0002-2267-4220>

<sup>b</sup>  <https://orcid.org/0000-0002-5787-2040>

The purpose of this study was to investigate the possibility to detect differentially two independent factors of interest, cortical thickness and intracortical porosity as diagnostically valuable determinants of bone fragility in osteoporosis. Synthetic solid phantoms modeling the cortical layer with the gradual variation of both factors were used. The very formulation of the problem suggested the need to apply pattern recognition methods, but unlike the classical classification problem, in this case, there was no need to determine the belonging of the object under study to any known class, but just to find the values of the factors, which were a-priori unknown. Soft tissues covering bones were considered as an aside factor, so the datasets were obtained for three thicknesses of the soft layer to assure the feasibility of the method for persons of different constitutions.

The raw data were presented by sets of ultrasonic signals acquired stepwise by surface profiling of the object in the pitch-catch mode. The discrete Fourier transform (DFT), one of the recognized methods of signal analysis, transforming the signals from time to frequency domains was used (Irrigaray et al., 2016). A set of statistical parameters was extracted from the set of magnitude signals, thus forming a set of features describing the object. Extracting statistical parameters from each object in the set, decision rules are created to be the instrument for the evaluation of parameters of interest in the examined objects.

## 2 PROPOSED APPROACH

The proposed approach for evaluating two factors-of-interest using ultrasonic signals datasets was based on pattern recognition principles. The evaluation method consisted of two parts: creating a set of decision rules from the data for a training set of phantoms and validating the set of decision rules by substitution the data for an examination specimen to make verify the correctness of the approach.

### 2.1 Bone Phantoms and Ultrasonic Data Acquisition

Bone models (phantoms) presented a set of bi-layer PMMA (polymethyl methacrylate) plates (Figure 1) with gradually varied overall thicknesses 2, 3, 4, 5 and 6 mm that corresponded to the bone cortical thickness CTh. The effect of intracortical porosity progressing from the in-bone channel was imitated by the regularly bottom-drilled holes. The volumetric porosity of the porous layer was constant at the level of 20%, but the gradual progress of porosity P from

zero to 100% of CTh was set by increasing the thickness of the porous layer PTh with a step of 1 mm.

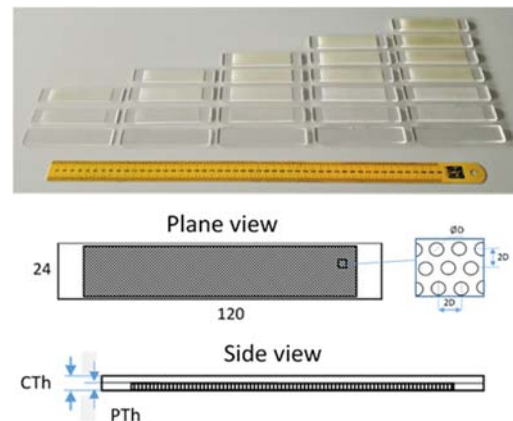


Figure 1: PMMA phantoms modeling the progression of osteoporosis in compact bone tissue: CTh – cortical thickness; PTh – thickness of the porous layer.

Ultrasonic signals were acquired by means of a custom-made scanning setup by stepwise profiling the upper surface of the phantoms covered by soft tissues with a profiling step of 3 mm (Figure 2).

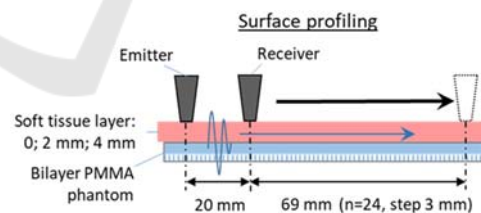
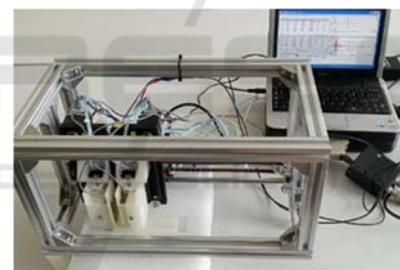


Figure 2: Acquisition of ultrasonic signals in phantoms: A – general view of ultrasonic setup, B – layout of experiment.

Totally acquired 24 signals formed so called ultrasonic spatiotemporal waveform profiles that served as the source material for pattern recognition (Figure 3). The profiles contained complex information on temporal (velocities) and energetic (attenuation) characteristics of different modes of ultrasound propagation in the objects. Commonly, it presents difficult to analyze those analytically using signals decomposition (Bochud et al., 2017), but the

pattern recognition approach provided an integral solution.

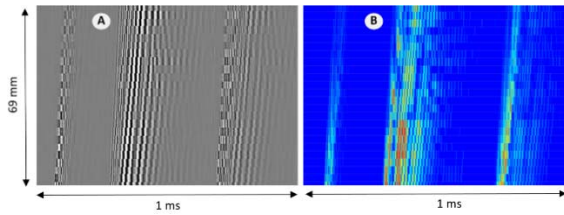


Figure 3: Examples of ultrasonic spatiotemporal waveform profiles in bone phantoms: A – normalized within each signal line; B – normalized upon the entire profile. The abscissa is ultrasonic time; the ordinate is profiling distance.

In one signal frame of a 1 ms duration, three frequency excitation responses were collected: HF at 500 kHz, LF at 100 kHz, and a chirp signal with frequency sweeping from 500 to 50 kHz. In this frequency range, different modes of ultrasonic guided waves manifested, including S0 and A0 Lamb waves.

### 2.2 Used Mathematical Method

The initial data set comprised raw ultrasonic signals obtained at three different frequency regimes of excitation (HF, LF, chirp) and forming the spatiotemporal waveform profiles that contained 24 stepwise acquired signals. The general structure of the initial data on objects (phantoms) is shown in Figure 4.

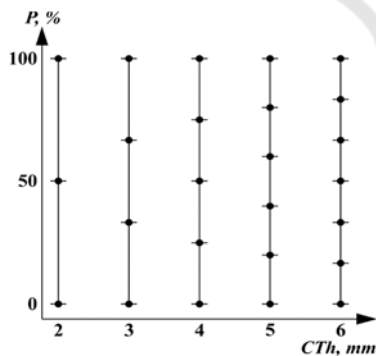


Figure 4: Data structure of source objects in the space of factors-of-interest CTh and P.

As the set of bi-layer phantoms consisted of gradually varied solid and porous layers with an increment of 1 mm, the objects' grid in the space of the factors-of-interest CTh and P was a non-orthogonal one that made an additional challenge for interpolation.

In this study, the method for evaluating of factors of interest used a pattern recognition approach

applied to ultrasonic signals after DFT processing (Sisojevs et al., 2022). The signal frame consisting of three frequency regimes was divided into three-time sub-frames. In each sub-frame, mathematical criteria were calculated. For this, the magnitude functions of the DFT signals received from the corresponding sub-frames were used. Then, for each object, mathematical criteria were calculated that presented various ratios between the envelope functions of signal magnitudes (Sisojevs et al., 2022). The total number of mathematical criteria for one sub-frame was 13, and considering three sub-frames in the time domain, the number of mathematical criteria for one object was 39.

After calculating the mathematical criteria for all objects in the training set, decision rules were built. In this case, mathematical criteria were used as attributes for pattern recognition rules. For decision rule creation, the bilinear interpolation of a patch of the surface was used (Sisojevs et al., 2022).

### 3 EXPERIMENTS

As part of the validation of the proposed approach, experiments were carried out to assess the total thickness of the bone phantom CTh and the thickness of the porous part P with a-priori known values of the soft tissue thickness. In the experiment, the soft tissue thicknesses were 0, 2 and 4 mm.

A separate experiment was carried out for each of the soft tissue thickness values. The experiment looked like this. Of all the scanned objects, one was selected for the test sample. The rest made up the training set. In this work, the method (Sisojevs et al., 2022) was used. For each object, the magnitudes of DFT signals were calculated for sub-frames in the signal time domain.

$$M(\omega) = \sqrt{(Re(\omega))^2 + (Im(\omega))^2}$$

where:

$$Re(\omega) = \sum_{t=t_{min}}^{t_{max}} s(t) \cdot \cos\left(\frac{2\pi \cdot t \cdot \omega}{t_{max} - t_{min}}\right)$$

and

$$Im(\omega) = \sum_{t=t_{min}}^{t_{max}} s(t) \cdot \sin\left(\frac{2\pi \cdot t \cdot \omega}{t_{max} - t_{min}}\right)$$

In the selected interval  $\omega$ , the values of three functions were calculated:

$$\begin{aligned} F_{max}(\omega) &= \max\{M(\omega)\}; \\ F_{avr}(\omega) &= \text{average}\{M(\omega)\} \text{ and} \\ F_{min}(\omega) &= \min\{M(\omega)\} \end{aligned}$$

Then, according to the values of these functions, mathematical criteria were calculated:

First criteria cr#1 is the number of  $\omega$  values that fulfill the condition

$$F_{max(\omega)} \geq average(F_{max(\omega)}), (cr\#1);$$

$$cr\#2 = \frac{\max(F_{min(\omega)})}{\max(F_{max(\omega)})}, cr\#3 = \frac{\max|dF_{max(\omega)}|}{\max(F_{max(\omega)})},$$

$$cr\#4 = \frac{\max|dF_{avr(\omega)}|}{\max(F_{max(\omega)})}, cr\#5 = \frac{\max|dF_{min(\omega)}|}{\max(F_{max(\omega)})},$$

where:

$$dF_{max}(\omega) = F_{max}(\omega) - F_{max}(\omega - 1).$$

$$dF_{avr}(\omega) = F_{avr}(\omega) - F_{avr}(\omega - 1).$$

$$dF_{min}(\omega) = F_{min}(\omega) - F_{min}(\omega - 1).$$

$$\begin{pmatrix} cr\#6 \\ cr\#7 \\ cr\#8 \end{pmatrix} = [W]^{-1} \cdot \begin{pmatrix} \sum_i \omega_i^2 \cdot F_{max}(\omega) \\ \sum_i \omega_i \cdot F_{max}(\omega) \\ \sum_i F_{max}(\omega) \end{pmatrix}$$

where:

$$[W] = \begin{pmatrix} \sum_i \omega_i^4 & \sum_i \omega_i^3 & \sum_i \omega_i^2 \\ \sum_i \omega_i^3 & \sum_i \omega_i^2 & \sum_i \omega_i \\ \sum_i \omega_i^2 & \sum_i \omega_i & \omega_{max} - \omega_{min} \end{pmatrix}$$

$$cr\#9 = \frac{\max(F_{avr}(\omega))}{\max(F_{max}(\omega))}$$

$$cr\#10 = \frac{S_{min}}{S_{max}}, cr\#11 = \frac{S_{avr}}{S_{max}},$$

$$cr\#12 = \frac{S_{max} - S_{avr}}{S_{max}}, cr\#13 = \frac{S_{avr} - S_{min}}{S_{max}}$$

where:

$$S_{min} = \frac{1}{\max\{F_{max}(\omega)\}} \cdot \sum_{\omega=\omega_{min}}^{\omega_{max}} F_{min}(\omega)$$

$$S_{avr} = \frac{1}{\max\{F_{max}(\omega)\}} \cdot \sum_{\omega=\omega_{min}}^{\omega_{max}} F_{avr}(\omega)$$

$$S_{max} = \frac{1}{\max\{F_{max}(\omega)\}} \cdot \sum_{\omega=\omega_{min}}^{\omega_{max}} F_{max}(\omega)$$

The interest parameter estimation method was based on the creation and use of decision rules. To create decision rules, piecewise linear interpolation was used for each of the parametric directions. As a result, the decision rule was represented as a piecewise bilinear function of two variables.

The use of a decision rule to evaluate an unknown object was reduced to the calculation of mathematical criteria and their comparison with the corresponding decision rules. In this case, the value of the criterion expanded to the interval  $\pm\epsilon$  (eps). The result of evaluation according to one rule is a set (segment) of possible correct answers. Figure 5 illustrates such a case.

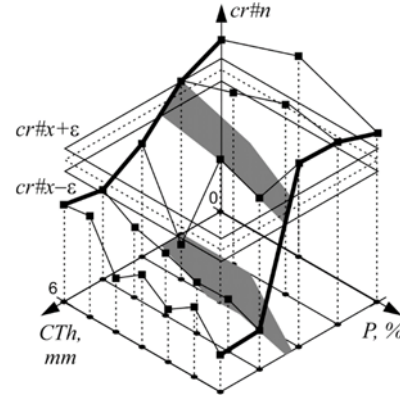


Figure 5: An example of using a single decision rule to evaluate an unknown object.

When using several decision rules, a sub-segment of possible answers is found that is included in the maximum number of initially found segments. It is this sub-segment that is taken as the final evaluation of the method used.

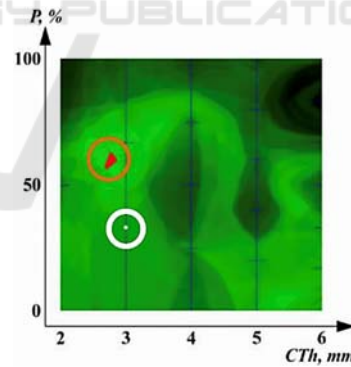


Figure 6: Result of evaluation of object with CTh = 3 mm and P = 33.3% (PTh = 1 mm), soft tissue thickness = 0 mm and eps = 25%.

After this estimate was obtained, this result was compared with the a-priori known values of CTh and P of this object. Within the framework of one experiment, each of the objects was chosen in turn as a test object.

Examples of how the method of the estimation factors-of-interest works are shown in Figures 6-8. In the figures, the red segment is the obtained estimate

of the non-test object by the method (Sisojevs et al., 2022), the white dot denotes the position of the test object.

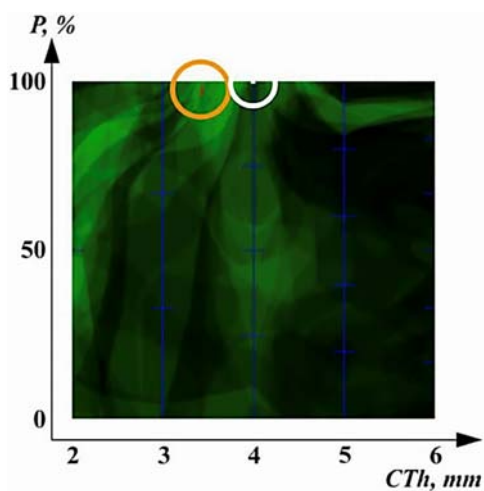


Figure 7: Result of evaluation of object with CTh = 4 mm, P = 100% (PTh = 4 mm), soft tissue thickness = 2 mm and eps = 25%.

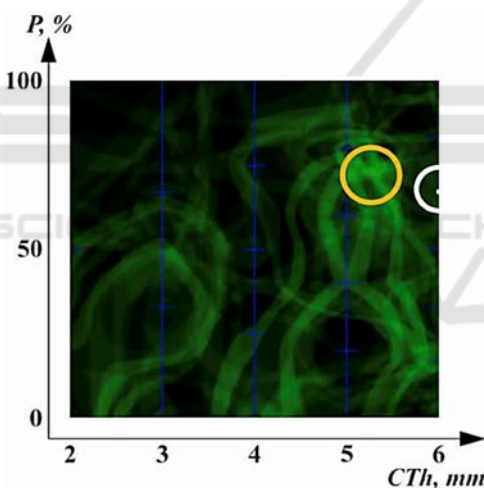


Figure 8: Result of evaluation of object with CTh = 6 mm, P = 66.6% (PTh = 4 mm), soft tissue thickness = 4 mm and eps = 5%.

### 3.1 Estimation Accuracy

The estimation accuracy in the experiment was determined for each of the factors-of-interest (CTh and P). The error was calculated as the modulus of the difference between the computed estimate of the factor's value and the a-priori known value of this factor in the object

The estimate of the error in determining CTh ranged from 0.0021 to 3.992 mm (i.e. between very precise and completely incorrect). The average

estimation error was in the range of 0.561 - 1.675 mm (depending on soft tissue thickness and eps value). After sorting the errors in ascending order, the distribution of errors is shown in Figure 9. The best results or the results showing the smallest deviation for CTh estimation are obtained with a value of the soft tissue thickness layer of 4 mm and 2 mm at eps=25% (average error 0.561 - 0.749 mm, maximum 1.606 - 2.532mm). Contrary, the worst results (the highest deviation) are obtained for the value of the soft tissue thickness layer 0 mm, regardless of the eps value (average error 1.372 - 1.675 mm, maximum 3.623 - 3.983 mm). If the acceptable diagnostic deviation threshold for CTh is 1.2 mm with a general range of its changes from 2 to 6 mm, then the number of correct estimations is 20 out of 25 or 80%.

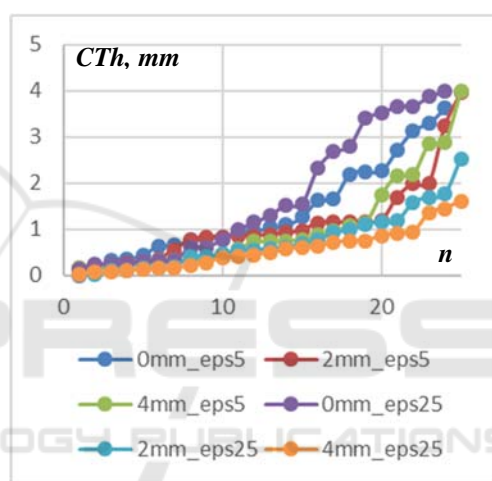


Figure 9: Distribution of errors for CTh estimations depending on the thickness of the soft tissue layer and eps.

The estimate of the error in determining the porosity ranged from 0 to 92.478%, i.e. from the lowest to the almost highest possible). The average estimation error was in the range of 21.736 - 31.162%. Depending on soft tissue thickness and eps value. After sorting the errors in ascending order, the distribution of errors for P is shown in Figure 10. The best results from the point of least deviation for porosity P were obtained with a soft tissue thickness layer 2 mm at eps=25% (average error 21.736%, maximum error 74.558%). At the same time, the parameters (thickness of soft tissue and eps) giving the worst performance in terms of accuracy are not indicated. If the acceptable diagnostic deviation threshold for P is 30% with a general range of its changes from 0 to 100% mm, then the number of correct estimations is 15 out of 25 or 60%. This shows that the accuracy of determining bone thickness CTh is somewhat better than that of its porosity P, using

DFT-based criteria applied to the ultrasonic signals related to the guided waves propagation.

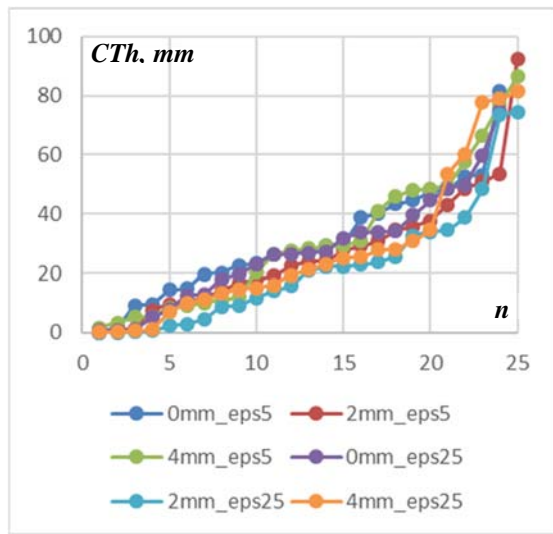


Figure 10: Distribution of porosity P estimation errors depending on the thickness of the soft tissue layer and eps.

## 4 CONCLUSIONS

The results of the experiments showed the potential effectiveness of the earlier proposed pattern recognition method (Sisojevs et al., 2022) in the tasks of determining the factors of interest in osteoporosis diagnostics (total thickness of the cortical bone and the degree of inner porosity), using ultrasonic surface profiling.

The use of only the DFT analysis does not give full agreement between the obtained estimates and the *a priori* predicted ones. The application of additional evaluation criteria based on the physical parameters of guided wave propagation may improve the reliability of the diagnosis.

The small number of available objects (bone phantoms) and the approximate nature of the mathematical criteria did not allow us to estimate the factors of interest with high accuracy. However, the results obtained demonstrated the prospects for using this method and increasing its accuracy with an increase in the number of objects with *a priori* known values of the factors.

## ACKNOWLEDGEMENTS

The study was supported by the research project of the Latvian Council of Science lzp-2021/1-0290

“Comprehensive assessment of the condition of bone and muscle tissues using quantitative ultrasound” (BoMUS).

## REFERENCES

- WHO Scientific Group on the Prevention and Management of Osteoporosis (2000: Geneva, Switzerland). (2003) *Prevention and management of osteoporosis: report of a WHO scientific group*. WHO Technical Report Series 921.
- Osterhoff G, Morgan EF, Shefelbine SJ, Karim L, McNamara LM, Augat P. (2016) Bone mechanical properties and changes with osteoporosis. *Injury*.; 47, *Suppl 2*: 11-20.
- Guglielmi G, Scalzo G. (2010) Imaging tools transform diagnosis of osteoporosis. *Diagnostic Imaging Europe*. 26: 7–11.
- Laugier P. (2008) Instrumentation for in vivo ultrasonic characterization of bone strength. *IEEE Trans Ultrason Ferroelectr Freq Control*; 55(6):1179-96.
- Tatarinov A, Egorov V, Sarvazyan N, Sarvazyan A. (2014) Multi-frequency axial transmission bone ultrasonometer. *Ultrasonics*. 54(5):1162-1169.
- Irrigaray, M. A. P., Pinto R.C. and Padaratz I. J (2016) A new approach to estimate compressive strength of concrete by the UPV method. *Revista IBRACON de Estruturas e Materiais* 9: 395-402.
- Bochud N, Vallet Q, Minonzio JG, Laugier P. (2017) Predicting bone strength with ultrasonic guided waves. *Sci Rep.*; 7 (3):43628.
- Sisojevs A., Tatarinov A., Kovalovs M., Krutikova O., Chaplinska A. (2022) An Approach for Parameters Evaluation in Layered Structural Materials based on DFT Analysis of Ultrasonic Signal. *Proceedings of the 11th International Conference on Pattern Recognition Applications and Methods, Volume 1: ICPRAM*, 307-314.